

Experimental study of toroidal and poloidal rotation induced by edge ergodization and electrode biasing in TEXTOR

S. Jachmich¹, M. Van Schoor¹, R.R. Weynants¹, Y. Xu¹, M. Jakubowski²,
M. Lehnen², M. Mitri², O. Schmitz² and the TEXTOR team

¹ *Laboratoire de Physique des Plasmas – Laboratorium voor Plasmafysica, Association 'Euratom-Belgian state', Ecole Royale Militaire – Koninklijke Militaire School, B-1000 Brussels, Belgium**

² *Institute for Energy Research – Plasma Physics, Forschungszentrum Jülich, EURATOM Association-FZJ, D-52425 Jülich, Germany**

* *Partner in the Trilateral Euregio Cluster (TEC)*

1. Introduction

Sheared plasma rotation is known to play a major role in the suppression of turbulence and concomitant confinement improvement. At TEXTOR this has been successfully demonstrated in electrode biasing discharges, where an externally driven current exerts a momentum on the plasma in the edge [1]. The recently installed dynamic ergodic divertor (DED) offers a unique way to impose rotation by the additional electron losses, which occur due to radial fieldline diffusion and enhanced radial conductivity [2-4]. In order to disentangle the underlying mechanism combined experiments have been carried out, where the radial conductivity in an ohmic discharge with an ergodized edge was probed by an externally driven radial current.

The experiments have been performed with the DED in the $m/n=6/2$ -configuration, where the width of the ergodic zone is of the order of a few centimetre. Positive and negative voltages have been applied between an electrode, which has been inserted beyond the last closed flux surface into the region of ergodized flux surfaces, and the toroidal belt limiter. Figure 1 gives an overview of a typical biasing discharge in DED-conditions. In a plasma discharge with $I_p=200\text{kA}$, $B_t=1.4\text{T}$, $q_{cyl}=4.5$, DED-currents of the order of 6kA were applied. During the flat-top phase the electrode voltage was slowly ramped up to obtain an I (V)-characteristic of the electrode. Radial profiles of electric field, poloidal and toroidal rotation were obtained by a Mach-probe mounted on a fast reciprocating probe drive at the times in the discharge as indicated in Fig.1(c).

2. Reduction of biasing driven radial current due to DED

In [5] a model for the cross-field current in stochastic fields has been proposed. This cross-field current j_{DED} , which results from the magnetic field line diffusion and the high electron mobility along field lines, can be expressed in terms of field line diffusion and the edge equilibrium profiles:

$$j_{DED} = 0.1e^2 D_{fl} n_e \sqrt{2 / \pi m_e T_e} \left(\frac{1}{en_e} \frac{\partial p_e}{\partial r} + \frac{2.1}{e} \frac{\partial T_e}{\partial r} \right) . \quad (1)$$

For a field line diffusion coefficient in the order of $D_{fl} \approx 10^{-6} - 10^{-5} \text{ m}^2/\text{m}$ we find this current density to be in the order of 6-60 A/m². In steady state and without electrode biasing, no

radial current can exist as the plasma would charge up infinitely, which requires an additional positive radial electric field to build up and an increase of the plasma potential to balance the electron losses at the edge. This is consistent with our observation that the electric field flattens in ohmic plasmas with the DED. Figure 2 shows floating potential profiles for various discharge conditions. The electric field is proportional to the gradient of the profiles. Probe measurements of the edge electron temperature has revealed that the contribution of the Te-gradient to the electric field is of order 0.5 kV/m which changes little in the examined pulses.

In the case of biasing in plasma discharges without perturbed magnetic flux surfaces, the biasing current has to be balanced by an ion-loss return current. Due to the ambipolarity constraint this current can be probed by the measurable biasing current. In references [6, 7] an analytic expression for the resulting electric field and cross-field conductivity has been derived:

$$E_r = E_{r,amb} + j_r^{bias} / \sigma_r^{neo} \quad , \quad (2)$$

$$\text{with } E_{r,amb} = \frac{1}{en_i} \frac{\partial p_i}{\partial r} - \frac{v_\phi}{v_\theta} \frac{-0.5}{eB_0} \frac{\partial T_i}{\partial r} \quad \text{and } \sigma_r^{neo} = \frac{m_i n_i}{B_0^2} (v_\theta + (1 + 2q^2)v_{i0})$$

where v_ϕ and v_θ are the toroidal and poloidal damping rates, respectively, and v_{i0} is the ion-neutral collision rate. In equation (2) we postulated $j_r^{bias} = j_{r,ion}$. A positive biasing current will lead to an ion loss current and the formation of an additional positive electric field. One should note that possible transport reduction effects via ExB-shear will alter the equilibrium profiles and hence the neo-classical ambipolar electric field will change. However, typically these effects are small compared to the externally imposed electric field.

In first order the electrode behaves like a Langmuir probe, i.e. the I(V)-characteristic of an electrode consists of an ion saturation branch and an exponential rising part (c.f. Fig. 3). For sufficiently high electrode voltages $V_E \geq 300-400\text{V}$, positive biasing exhibits a phenomenon known as bifurcation. In this study we have restricted ourselves to the study at modest biasing voltages. The rather small ion saturation current of 20 A makes it difficult to impose significant negative electric fields using biasing. In figure 3 current/voltage-characteristics for cases with and without DED and for different toroidal magnetic field and plasma current directions are shown. First one notes that the floating potential of the electrode is shifted in the DED-discharges towards positive voltages, which is due to the change in the plasma potential caused by the edge electron losses. However, the shift of the plasma potential is not sufficient to explain the large drop in the electrode current I_E for large electrode voltages once the DED is energised. For instance, for $V_E=210\text{ V}$ one would expect about 180 to 240 A electrode current, but for the equivalent voltage of 300 V only 150 A are drawn. This is due to the reduction of the return current by the additional electron loss current. Assuming a toroidal surface area of 32 m² at the LCFS the loss current according to Eq. (1) would be sufficient to explain the smaller electrode currents.

The DED imposes a three-dimensional magnetic field structure. As a result the local connection length and formation of magnetic islands depend on the toroidal and poloidal location of the electrode and the fast probe. In order to study whether the externally driven

radial current density is toroidally uniform and that the drop in I_E with increasing I_{DED} is not due to a local connection to one of the toroidal limiter blades, the plasma current and magnetic field has been reversed. The helicity is preserved, but the relative location of the electrode in the magnetic field pattern is varied. As figure 3 shows also for the reversed I_p/B_t -case we find a strong reduction of the electron current. In fact, the $I(V)$ -characteristics are similar for both magnetic field directions.

3. Edge profiles during electrode biasing and DED

Figures 4 and 5 show the corresponding profiles of the parallel and perpendicular flow, which are directly measured by the Mach probe. Parallel and perpendicular refer to the magnetic field direction in the unperturbed case, which are related to the toroidal and poloidal rotation via the pitch angle. For above discharge parameter, the angle is of order $4-5^\circ$, the toroidal rotation is approximately represented by the parallel flow and the poloidal by the perpendicular flow. One can assume that this is still valid during the DED-phase, since the probe collectors (4mm x 4mm) are a rather macroscopic object compared to the size scale of the magnetic field line diffusion variation. The first striking observation is that on one hand the DED leads to a drastic change of the parallel flow. The biasing on the other hand has a more pronounced effect on the poloidal rotation. As seen in Fig. 5 the poloidal rotation flattens once the DED is turned on as it can be expected from the electric field profile. The additional electrode current leads to an additional increase of the poloidal rotation in agreement with measured higher electric fields. However, the poloidal rotation is much less localised during the DED, which results in lower ExB shearing rates and detrimental effects on turbulence suppression. We would like to remark that this is in contrast to the very specific discharge conditions for the TEXTOR improved confinement mode, for which indications of ExB shearing rate changes have been found [8].

4. Summary

In biasing experiments the externally imposed current is lowered by the additional electron losses caused by magnetic field perturbation and an increase in the plasma potential. The radial electric field and rotation profiles change accordingly. As a consequence, edge magnetic field perturbations in biasing experiments will result in lower ExB shearing rates, which can be recovered only to some extent by operating at higher electrode voltages.

- [1] R.R. Weynants *et al.*, Nuclear Fusion **32** (1992), 837.
- [2] K.H. Finken *et al.*, Plasm. Phys. Contr. Fus. **46** (2004), B143.
- [3] B. Unterberg *et al.*, Journ. Nucl. Material **363-365** (2007), 698.
- [4] Y. Xu *et al.*, Phys. Rev. Lett. **97** (2006), 165003.
- [5] I. Kaganovich *et al.*, Phys. Plasm. **5** (1998), 3901.
- [6] J. Cornelis *et al.*, Nuclear Fusion **34** (1994), 171.
- [7] M. Van Schoor *et al.*, Journ. Nucl. Material **290-293** (2001), 962.
- [8] J. Coenen *et al.*, this conference proceeding.

Figures

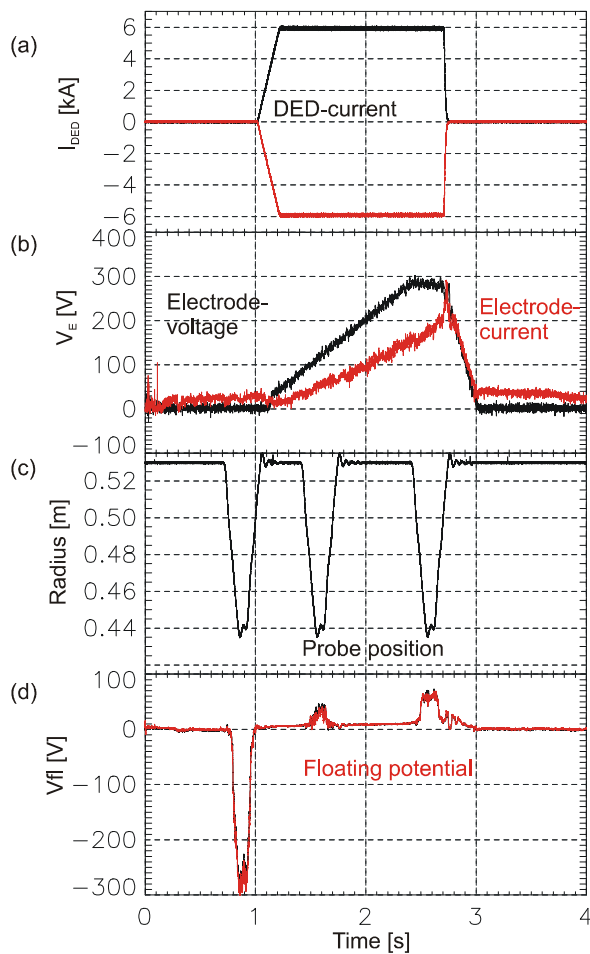


Fig. 1: Biasing discharge with edge ergodization showing time traces of (a) magn. field perturbation current, (b) electrode voltage and current, (c) radial probe position and (d) floating potential.

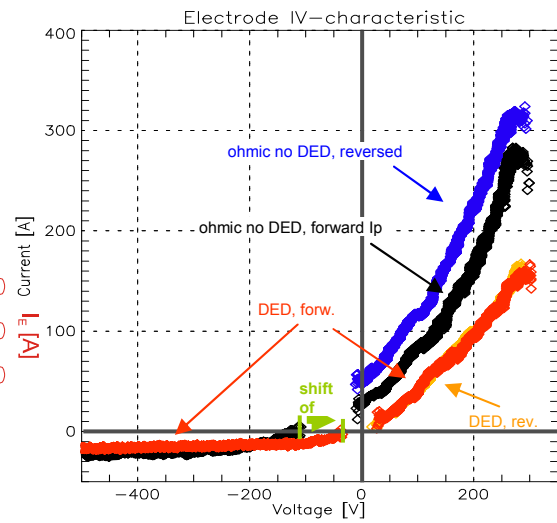


Fig. 3: I(V)-characteristics of electrode for various discharge conditions.

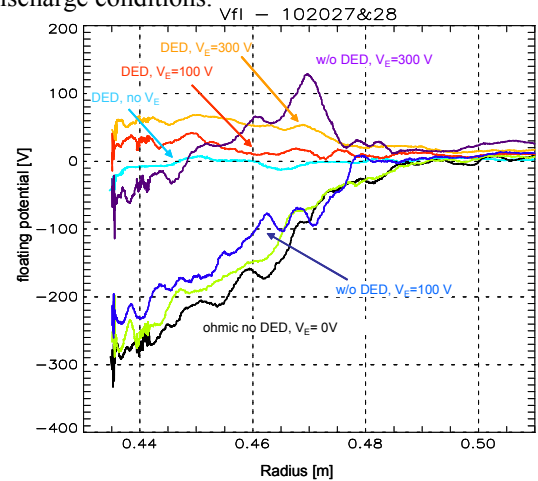


Fig. 2: Floating potential profiles for ohmic (black, green), DED-only (cyan) and biasing without (blue, purple) and with DED (red, yellow).

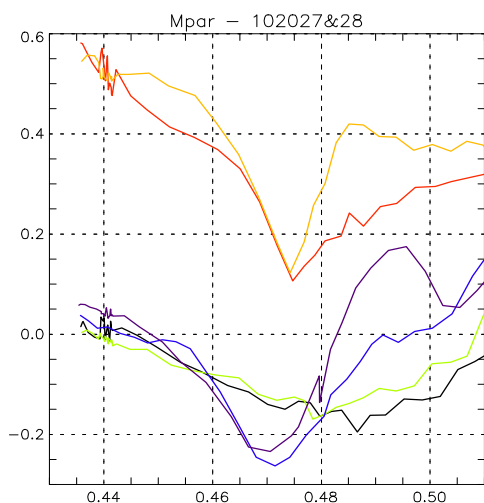


Fig. 4: Profiles of parallel flow. The colour codes correspond to those in figure 3.

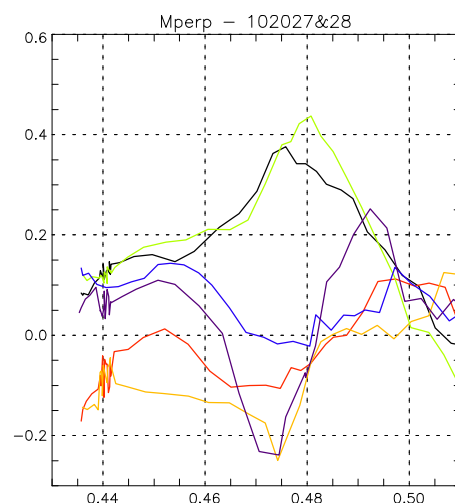


Fig. 5: Profiles of perpendicular flow. The colour codes correspond to those in figure 3.